

NACA RM L50H25B



# RESEARCH MEMORANDUM

A SMALL-SCALE INVESTIGATION OF "M" AND "W" WINGS

AT TRANSONIC SPEEDS

By George S. Campbell and William D. Morrison, Jr.

Langley Aeronautical Laboratory  
Langley Air Force Base, Va.

CLASSIFICATION CANCELLED

Authority NACA Res. abs. Data 11-14-56  
+ RN-109  
By NB 11-30-56 See \_\_\_\_\_

CLASSIFIED DOCUMENT

This document contains classified information affecting the National Defense of the United States within the meaning of the Espionage Act, USC 5031, and the transmission or communication of its contents in any manner to an unauthorized person is prohibited by law. Information so classified is to be furnished only to persons in the military and naval services of the United States, appropriate civilian officials and employees of the Federal Government who have a legitimate interest therein, and to United States citizens of known loyalty and discretion who of necessity must be informed thereof.

## NATIONAL ADVISORY COMMITTEE FOR AERONAUTICS

WASHINGTON

October 2, 1950

TO: NATIONAL ADVISORY COMMITTEE FOR AERONAUTICS  
FROM: NACA MEMORANDUM REPORT NO. 1083

## NATIONAL ADVISORY COMMITTEE FOR AERONAUTICS

## RESEARCH MEMORANDUM

A SMALL-SCALE INVESTIGATION OF "M" AND "W" WINGS  
AT TRANSONIC SPEEDS

By George S. Campbell and William D. Morrison, Jr.

## SUMMARY

An aerodynamic investigation has been conducted in the Langley high-speed 7- by 10-foot tunnel in order to compare the characteristics of wings of "M" and "W" plan forms with those of a wing having conventional sweepback. Three semispan wings were investigated at Mach numbers from 0.60 to 1.08 at Reynolds numbers of the order of 600,000. The wings were of aspect ratio 6 and taper ratio 0.6 and had NACA 65A009 airfoil sections; the quarter-chord lines were swept  $45^\circ$ . In addition to the lift, drag, pitching-moment, and bending-moment data, changes in local wing incidence measured under simulated air loads are presented. Theoretical span loadings were calculated at a Mach number of 0.70.

The M- and W-wings did not exhibit the large forward aerodynamic-center shift at low lift coefficients that was found for the conventional sweptback wing near a Mach number of unity. Likewise, a more regular variation of lift slope with Mach number was obtained for the wings of M and W plan form. Moreover, the W-wing showed practically no change in local wing incidence under load; the angular deflection of the M-wing was of smaller magnitude and opposite sign from that of the sweptback wing. In contrast to the improved stability and structural characteristics noted for the M and W plan forms, the lift-drag ratios of these wings, particularly the W-wing, were generally lower than the values for the sweptback wing. The differences in lift-drag ratio were most pronounced in the vicinity of a Mach number of 0.95. The zero-lift drag rise of the M- and W-wings was earlier and slightly more pronounced than for the sweptback wing. At low supersonic Mach numbers; the minimum drag was about 0.006 higher for the M- and W-wings than for the sweptback wing.

## INTRODUCTION

The use of "M" and "W" plan forms was originally advanced in Germany as one method of minimizing the undesirable pitching-moment characteristics frequently encountered near stall on highly sweptback wings, and at least one low-speed investigation (reference 1) conducted in this country has verified this idea. Research on this type of plan form was not pursued further because it was thought that the many wing-panel junctures inherent in this type of wing would diminish the favorable effects of sweep at high speeds. Recently, however, renewed interest has been kindled in this type of plan form as a result of certain structural advantages, particularly regarding wing deflection under load.

Accordingly, an investigation has been conducted in the Langley high-speed 7- by 10-foot tunnel to determine the transonic aerodynamic characteristics of an M- and a W-plan-form wing with panel sweeps of  $45^\circ$  and to compare these characteristics with those of a conventional swept-back plan form. Static loads were also applied to these wings to determine the wing twist under load.

This paper presents force and moment results for the three wings that were investigated as reflection-plane models over a Mach number range from 0.60 to 1.08. Estimates of the effect of wing deformation on lift-curve slope were made from the static-load tests. In addition, results from theoretical calculations have been compared with experimental values.

## COEFFICIENTS AND SYMBOLS

$C_L$	lift coefficient	$\left( \frac{\text{Twice semispan lift}}{qS} \right)$
$C_D$	drag coefficient	$\left( \frac{\text{Twice semispan drag}}{qS} \right)$
$C_m$	pitching-moment coefficient referred to $0.25\bar{c}$	$\left( \frac{\text{Twice semispan pitching moment}}{qS\bar{c}} \right)$
$C_B$	bending-moment coefficient about root-chord line	$\left( \frac{\text{Root bending moment}}{q \frac{S}{2} \frac{b}{2}} \right)$
$\Delta C_D$	drag coefficient due to lift	$(C_D - C_{D_{\min}})$

$\Delta H$	total-pressure loss in wake, pounds per square foot
$q$	effective dynamic pressure over span of model, pounds per square foot $(\rho V^2/2)$
$\rho$	mass density of air, slugs per cubic foot
$V$	free-stream velocity, feet per second
$S$	twice wing area of semispan model, square feet
$\bar{c}$	mean aerodynamic chord of wing using theoretical tip, feet $\left( \frac{2}{S} \int_0^{b/2} c^2 dy \right)$
$c$	local wing chord, feet
$y$	spanwise distance from wing root, feet
$z$	distance above wake center line, feet
$b$	twice span of semispan model, feet
$M$	effective Mach number over span of model
$M_L$	local Mach number
$R$	Reynolds number of wing based on $\bar{c}$
$\alpha$	angle of attack, degrees
$y_{cp}$	lateral center of pressure, percent semispan $\left( 100 \frac{C_B}{C_L} \right)$
$C_{L\alpha}$	wing lift-curve slope per degree $(\partial C_L / \partial \alpha)$
$c_{l\alpha}$	section lift-curve slope per degree $(\partial c_l / \partial \alpha)$
$\alpha_D$	change in local wing incidence due to wing deflection under air load, measured in plane parallel to plane of symmetry, degrees
$L$	total wing lift, pounds
$L_D$	change in lift from deflection, positive if gain; a first-order correction with respect to $L_R$

- K span-loading coefficient ( $c_l c / C_{L_{cav}}$ )  
 $c_l$  local lift coefficient ( $l / q c \, dL / dy$ )  
 $c_{av}$  mean wing chord, feet ( $S / b$ )

Subscripts:

- R rigid-wing value  
 E elastic or experimental value  
 min minimum value

MODELS AND METHODS

The steel semispan-wing models were of aspect ratio 6 and taper ratio 0.6 and had NACA 65A009 airfoil sections parallel to the free stream. The quarter-chord lines of the wings were swept  $45^\circ$  and the M and W plan forms had sweep breaks at the midsemispan position. A drawing of the plan forms tested is presented as figure 1.

The investigation was conducted in the Langley high-speed 7- by 10-foot tunnel. In order to test the semispan models in a region outside the tunnel boundary layer, a reflection plane was mounted about 3 inches from the tunnel wall, as shown in figure 2. The reflection-plane boundary-layer thickness was such that a value of 95 percent of free-stream velocity was reached at a distance 0.16 inch from the surface at the balance center line for all test Mach numbers. This thickness represented a distance of 3 percent semispan for the models tested.

At Mach numbers below 0.95, there was practically no velocity gradient in the vicinity of the reflection plane. At higher Mach numbers, however, the presence of the reflection-plane setup created a high-local-velocity field which allowed testing the small models up to  $M = 1.08$  before choking occurred in the tunnel. The variation of local Mach number in the vicinity of the reflection plane at these higher Mach numbers is shown in figure 3. Effective Mach number was obtained from contour charts similar to those of figure 3 by the relationship

$$M = \frac{2}{S} \int_0^{b/2} \int_{L.E.}^{T.E.} M_2 \, dx \, dy$$

For the models tested, a Mach number gradient of generally less than 0.02

was obtained between Mach numbers of 0.95 and 1.04, increasing to about 0.06 at the highest test Mach number of 1.08. It will be noted that the Mach number gradient is principally chordwise.

Force and moment measurements were made for the wings at Mach numbers from 0.60 to 1.08; the variation of average Reynolds number with Mach number for these tests is shown in figure 4. Data were obtained by using a strain-gage balance system mounted outside the tunnel. The sweptback and W-wings were tested with the quarter mean aerodynamic chord located at the balance center line. However, because of mechanical limitations, the pitching moments of the M-wing were measured about the 53 percent mean aerodynamic chord and were transferred to the quarter mean aerodynamic chord. The lateral axis of the balance was located at the root chord, so that transfers to the bending moments were unnecessary. Leakage through a small clearance gap between the turntable and wing root was restricted by means of a sponge seal attached to the wing butt and wiping against the inside of the reflection plane.

In addition to the force measurements, limited wake surveys were made at a position 4.2 inches behind the quarter mean aerodynamic chord of the W-wing using a survey rake with a tube spacing of 1/8 inch.

In view of the small size of the models relative to the tunnel test section, jet-boundary and blockage corrections were believed to be insignificant and hence were not applied.

## RESULTS AND DISCUSSION

### Presentation of Results

Results from the high-speed wind-tunnel investigation, from static-deflection measurements and from theoretical loading calculations, are summarized in the following figures:

	Figures
Basic aerodynamic data . . . . .	5 to 8
Summary of aerodynamic characteristics . . . . .	9
Comparison of aerodynamic characteristics at representative Mach numbers . . . . .	10
Effects of wing deformation . . . . .	11
Theoretical span loadings . . . . .	12

### Lift and Drag Characteristics

Lift and lateral center of pressure.- In comparing the lift characteristics of the M- and W-wings with those of the conventional sweptback wing (hereafter referred to as a  $\Lambda$ -wing), it can be seen that, in general, a more gradual variation of lift-curve slope near zero lift with Mach number was evident for the wings of composite plan form. (See fig. 9.) In fact, the W-plan-form wing showed an almost constant value of lift-curve slope (0.060) throughout the test Mach number range. At most Mach numbers, the M-wing had an appreciably higher lift slope near zero lift than either of the other plan forms.

For the  $\Lambda$ -wing at low lifts, an inboard movement of the lateral center of pressure occurred at the higher Mach numbers, apparently as a result of the tip separation frequently observed for the thicker sweptback wings at transonic speeds. In comparison, it may be seen from the bending-moment data of figures 6, 7, and 9 that the lateral center of pressure for both the M- and W-plan forms remained practically constant throughout the lift-coefficient and Mach number range of the present tests.

Drag.- The value of minimum drag coefficient is essentially equal for the  $\Lambda$ -, M-, and W-wings up to a Mach number of 0.90. (See fig. 9.) An initial zero-lift drag rise occurred at about 0.95 Mach number for the  $\Lambda$ -wing, and an earlier and slightly more pronounced drag rise was observed for the M and W plan forms. It is interesting to note that at low-supersonic Mach numbers, the minimum drag coefficient was about 0.006 higher for the M- and W-wings than for the  $\Lambda$  plan form. Nevertheless, a large proportion of the sweep effect is realized inasmuch as estimates made from unpublished data for a comparable unswept wing with the same streamwise thickness indicate an increment of about 0.040 attributable to sweepback. These minimum-drag results are in qualitative agreement with those of the recent investigation of reference 2.

A comparison of drag due to lift at a moderate lift coefficient, 0.3, (fig. 9) indicates that the W-wing had the highest value of drag due to lift throughout most of the test Mach number range. After consideration of probable boundary-layer drain, especially in the light of theoretical loadings presented in figure 12, a region of separated flow in the vicinity of the panel juncture of the W-wing might be suspected as the cause of the high drag due to lift for this wing. Total-pressure surveys at an angle of attack of  $4^\circ$  (fig. 8) provided evidence of pronounced separation in the vicinity of the juncture for the W-wing.

Lift-drag ratio.- Although both the  $\Lambda$ - and M-wings had a maximum lift-drag ratio of about 16 at lower Mach numbers, the M-wing showed a substantial reduction in  $(L/D)_{\max}$  above a Mach number of 0.85, and

at  $M = 0.95$ , the maximum lift-drag ratio of the M-wing was approximately 30 percent lower than that of the  $\Lambda$  plan form. The W-wing had the lowest value of  $(L/D)_{\max}$  throughout the Mach number range, apparently as a result of the juncture separation indicated by the wake survey. Maximum lift-drag ratios were about 20 percent lower for the wings of composite plan form than for the sweptback wing at the highest test Mach numbers.

#### Pitching-Moment Characteristics

At the lower Mach numbers (0.60 to 0.80) and near zero lift, aerodynamic-center locations of 20, 23, and 31 percent mean aerodynamic chord were realized for the M-,  $\Lambda$ -, and W-plan-form wings, respectively (fig. 9). The aerodynamic center for the  $\Lambda$ -wing in the low-lift range shifted forward about 50 percent of the mean aerodynamic chord between Mach numbers of 0.95 and 1.03 (fig. 9). This significant trend, which is probably attributable to the previously discussed tip separation, was not observed to any appreciable extent for either the M or W plan form.

Moreover, the extreme irregularity of the pitching moment with lift for the  $\Lambda$ -wing at the higher Mach numbers was considerably reduced with the M-wing, and still further improvement was indicated for the W-wing. (See comparison in fig. 10.) For the Reynolds numbers of the present tests, the W-wing generally appeared to have the most stable tendencies at the higher lifts.

#### Effects of Wing Deformation

In order to determine the relative flexibility of the three plan forms as mounted in the present tests, the wings of this investigation were statically loaded at two spanwise points on the quarter-chord line, and the resulting change in local wing incidence was measured at several spanwise stations. The concentrated loadings were chosen to approximate the theoretical span loadings which are presented subsequently.

The W-wing showed relatively little angular deflection under load (fig. 11) in comparison with the deflection of the conventional sweptback wing. The M-wing exhibited a deflection of smaller magnitude and opposite sign from that of the sweptback wing.

In order to obtain a first-order estimate of the effects of wing deformation on the lift results previously discussed, the following expression for rigid-wing lift in terms of elastic (measured) wing lift has been derived in the appendix:

$$C_{LR} = C_{LE} \left[ 1 - q \frac{S}{2} C_{L\alpha_E} \int_0^1 K_R \frac{\alpha_D}{L/2} d\left(\frac{y}{b/2}\right) \right] \quad (1)$$

It has been found that the effect of the loading term in equation (1) is sufficiently small that reliable lift corrections may be obtained throughout the test Mach number range by using the theoretical incompressible loading. It is seen (fig. 11) that for the 9-percent-thick steel wings tested, the maximum elastic lift correction was less than about 8 percent. Application of the elastic corrections brought the lift-curve slopes closer together at each test Mach number (fig. 11), but the trends with Mach number were not materially affected. Theoretical values of lift slope shown subsequently were essentially equal for the three wings so that the aeroelastic corrections have helped to confirm this theoretical observation.

Strip-theory estimates of rigid-wing lateral center of pressure and aerodynamic center for the  $\Lambda$ -wing at 0.90 Mach number indicated aeroelastic corrections of 2 percent semispan and 5 percent mean aerodynamic chord, respectively. However, it has been shown in reference 3 that while strip theory provides a satisfactory prediction of elastic lift corrections, the shift in center of span loading is considerably overestimated. In the light of the general unreliability of such corrections, rigid-wing centers of pressure have not been estimated for the wings tested.

#### COMPARISON WITH THEORY

In order to calculate the aerodynamic characteristics of the  $\Lambda$ -, M-, and W-wings at a Mach number of 0.70, each wing was replaced by a system of 20 equally spaced horseshoe vortices placed along the quarter-chord line of an equivalent incompressible plan form obtained from the Prandtl-Glauert transformation. Application of the tangent-flow boundary condition at 20 control points located along the three-quarter chord provided a set of 10 simultaneous equations in the 10 unknown circulation strengths. Solution of the equations provided theoretical values of lift-curve slope, lateral center of pressure, and aerodynamic center at Mach number 0.70 that are compared with the experimental values in the following table:

Parameter	Wing	Experimental	Theoretical
* $\partial C_L / \partial \alpha$	$\left\{ \begin{array}{l} \Lambda \\ M \\ W \end{array} \right.$	0.060	0.069
		.064	.071
		.060	.071
$y_{cp}$	$\left\{ \begin{array}{l} \Lambda \\ M \\ W \end{array} \right.$	47	47
		46	43
		44	44
$\partial C_m / \partial C_L$	$\left\{ \begin{array}{l} \Lambda \\ M \\ W \end{array} \right.$	.02	-.03
		.05	-.02
		-.09	-.07

\*Experimental lift slopes corrected for wing deformation.

It is seen that the theoretical lift-curve slopes are considerably larger than the experimental values. However, a section slope of 0.110 ( $2\pi$  per radian) was assumed by means of the three-quarter-chord concept in the theoretical method. The best available estimate of the low-speed section slope for sections normal to the quarter chord of the  $\Lambda$ -wing appears to be about 0.092 at a Reynolds number of 600,000. (See reference 4.) Results presented in reference 5 indicate that such a difference of section lift-curve slope would reduce the theoretical lift slope for the  $\Lambda$ -wing to 0.060, which is equal to the experimental value. A similar reduction in theoretical lift slope resulting from low Reynolds number might be expected for the M and W plan forms.

The agreement of theoretical and experimental lateral centers of pressure is satisfactory. Although the trend in aerodynamic-center position is indicated qualitatively by theory, the magnitude of the difference is underestimated.

The theoretical span-load distributions for the  $\Lambda$ -, M-, and W-wings at a Mach number of 0.70 are presented in figure 12. The load distribution for the W-wing is of a type that is particularly conducive to the pile-up of boundary-layer air near the plan-form break; for the M-wing, a similar pile-up would be expected at the root section. Previously discussed wake surveys made behind the W-wing have shown that this boundary-layer accumulation resulted in a severe separation in the vicinity of the panel juncture.

## CONCLUSIONS

The results of a small-scale investigation of a sweptback wing and two wings having "M" and "W" plan forms at Mach numbers between 0.60 and 1.08 indicate that:

1. The M- and W-wings did not exhibit the large forward aerodynamic-center movement at low lift coefficients that was found for the conventional sweptback wing near a Mach number of unity. Likewise, a more regular variation of lift slope with Mach number was obtained for the wings of M and W plan forms.

2. Moreover, the W-wing showed practically no change in local wing incidence under load; angular deflection of the M-wing was of smaller magnitude and opposite sign from that of the sweptback wing.

3. In contrast to the improved stability and structural characteristics noted for the M and W plan forms, the lift-drag ratios of these wings, particularly the W-wing, were generally lower than the values for the sweptback wing. The differences in lift-drag ratios were most pronounced in the vicinity of a Mach number of 0.95.

4. The zero-lift drag rise of the M- and W-wings was earlier and slightly more pronounced than for the sweptback wing. At low-supersonic Mach numbers, the minimum drag was about 0.006 higher for the M- and W-wings than for the sweptback wing.

Langley Aeronautical Laboratory  
National Advisory Committee for Aeronautics  
Langley Air Force Base, Va.

## APPENDIX

## DERIVATION OF EXPRESSION FOR RIGID-WING LIFT

Rigid-wing lift is related to the experimental value by the expression

$$L_R = L_E - L_D \quad (A1)$$

where

$$L_D = q \int_{-b/2}^{b/2} c_{l_{\alpha}} \alpha_D^c dy \quad (A2)$$

The product  $c_{l_{\alpha}} c$  in terms of the span-loading coefficient  $K$  is

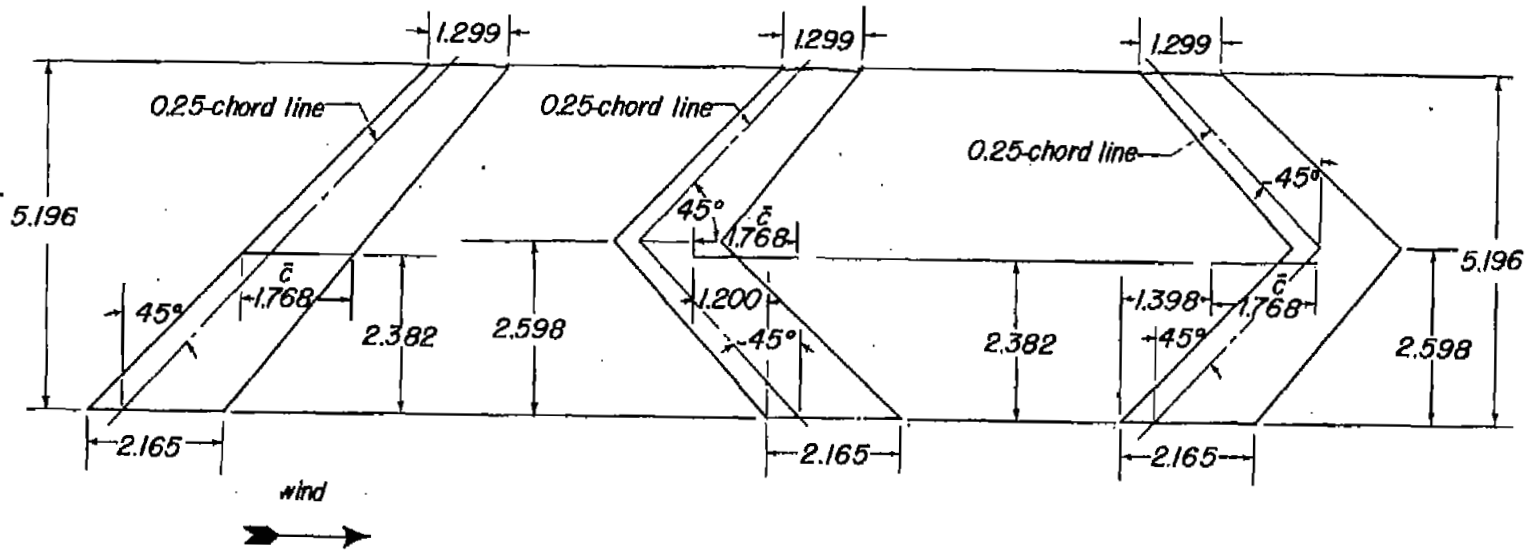
$$c_{l_{\alpha}} c = C_{L_{\alpha E}} \frac{S}{b} K_E \quad (A3)$$

For a first-order correction to elastic lift, the elastic-loading parameter  $K_E$  may be replaced by the theoretical rigid-wing value  $K_R$ . Substitution of equations (A2) and (A3) into (A1) provides a formula for the rigid-wing lift in terms of the elastic (measured) value:

$$C_{L_R} = C_{L_E} \left[ 1 - q \frac{S}{2} C_{L_{\alpha E}} \int_0^1 K_R \frac{\alpha_D}{L/2} d\left(\frac{y}{b/2}\right) \right] \quad (A4)$$

## REFERENCES

1. Purser, Paul E., and Spearman, M. Leroy: Wind-Tunnel Tests at Low Speed of Swept and Yawed Wings Having Various Plan Forms. NACA RM L7D23, 1947.
2. Katz, Ellis, Marley, Edward T., and Pepper, William B.: Flight Investigation at Mach Numbers from 0.8 to 1.4 to Determine the Zero-Lift Drag of Wings with "M" and "W" Plan Forms. NACA RM L50G31, 1950.
3. Frick, C. W., and Chubb, R. S.: The Longitudinal Stability of Elastic Swept Wings at Supersonic Speed. NACA TN 1811, 1949.
4. Loftin, Laurence K., Jr., and Smith, Hamilton A.: Aerodynamic Characteristics of 15 NACA Airfoil Sections at Seven Reynolds Numbers from  $0.7 \times 10^6$  to  $9.0 \times 10^6$ . NACA TN 1945, 1949.
5. Polhamus, Edward C.: A Simple Method of Estimating the Subsonic Lift and Damping in Roll of Sweptback Wings. NACA TN 1862, 1949.



*Tabulated Wing Data , A-Wing*

Sweep	45°
Aspect ratio	6
Taper ratio	0.6
Airfoil section parallel to free stream	NACA 65A009
Area (twice semispan)	0.125 sq ft

*Tabulated Wing Data , M-Wing*

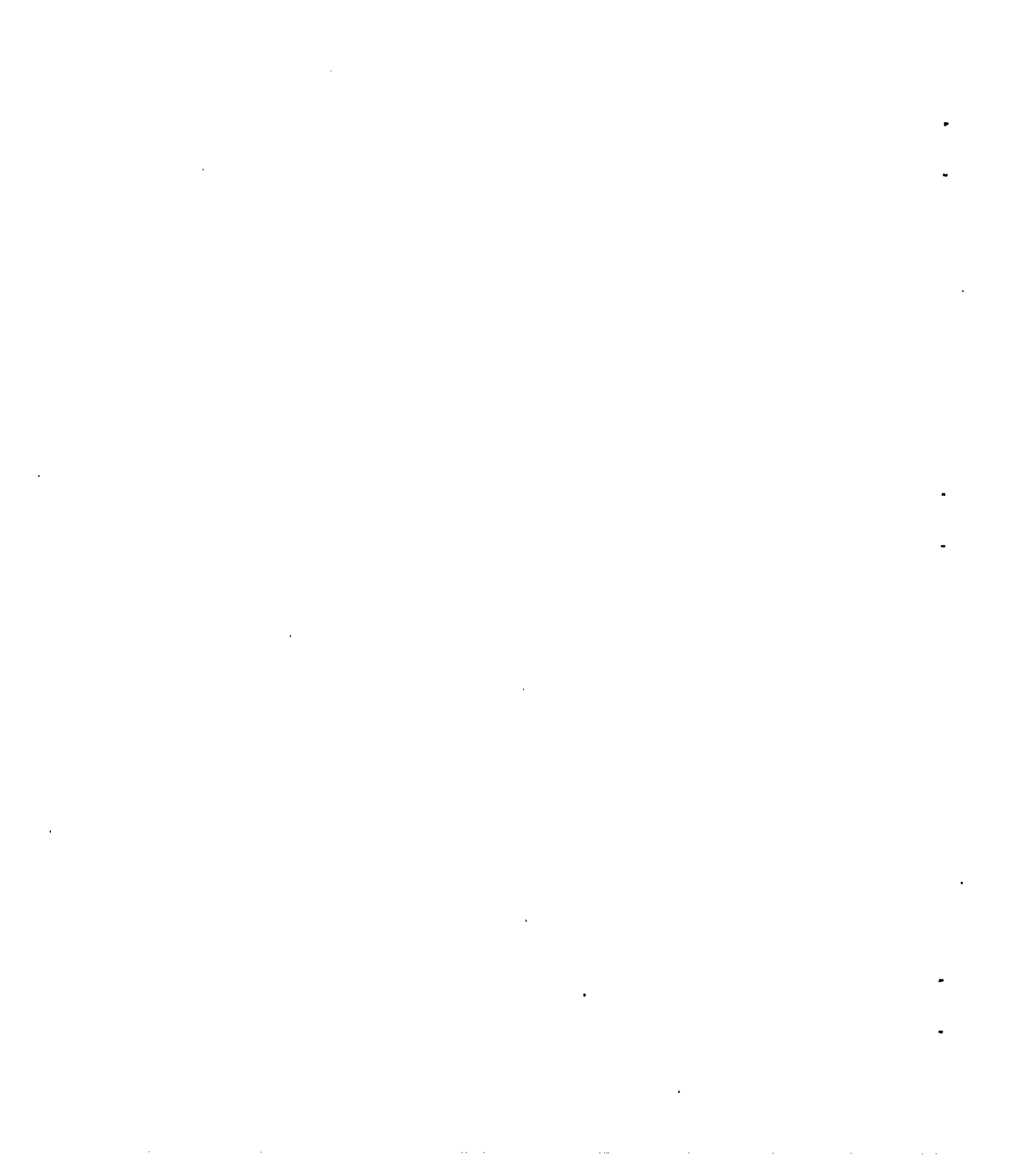
Sweep of inboard panel	-45°
Sweep of outboard panel	45°
Aspect ratio	6
Taper ratio	0.6
Airfoil section parallel to free stream	NACA 65A009
Area (twice semispan)	0.125 sq ft

*Tabulated Wing Data , W-Wing*

Sweep of inboard panel	45°
Sweep of outboard panel	-45°
Aspect ratio	6
Taper ratio	0.6
Airfoil section parallel to free stream	NACA 65A009
Area (twice semispan)	0.125 sq ft



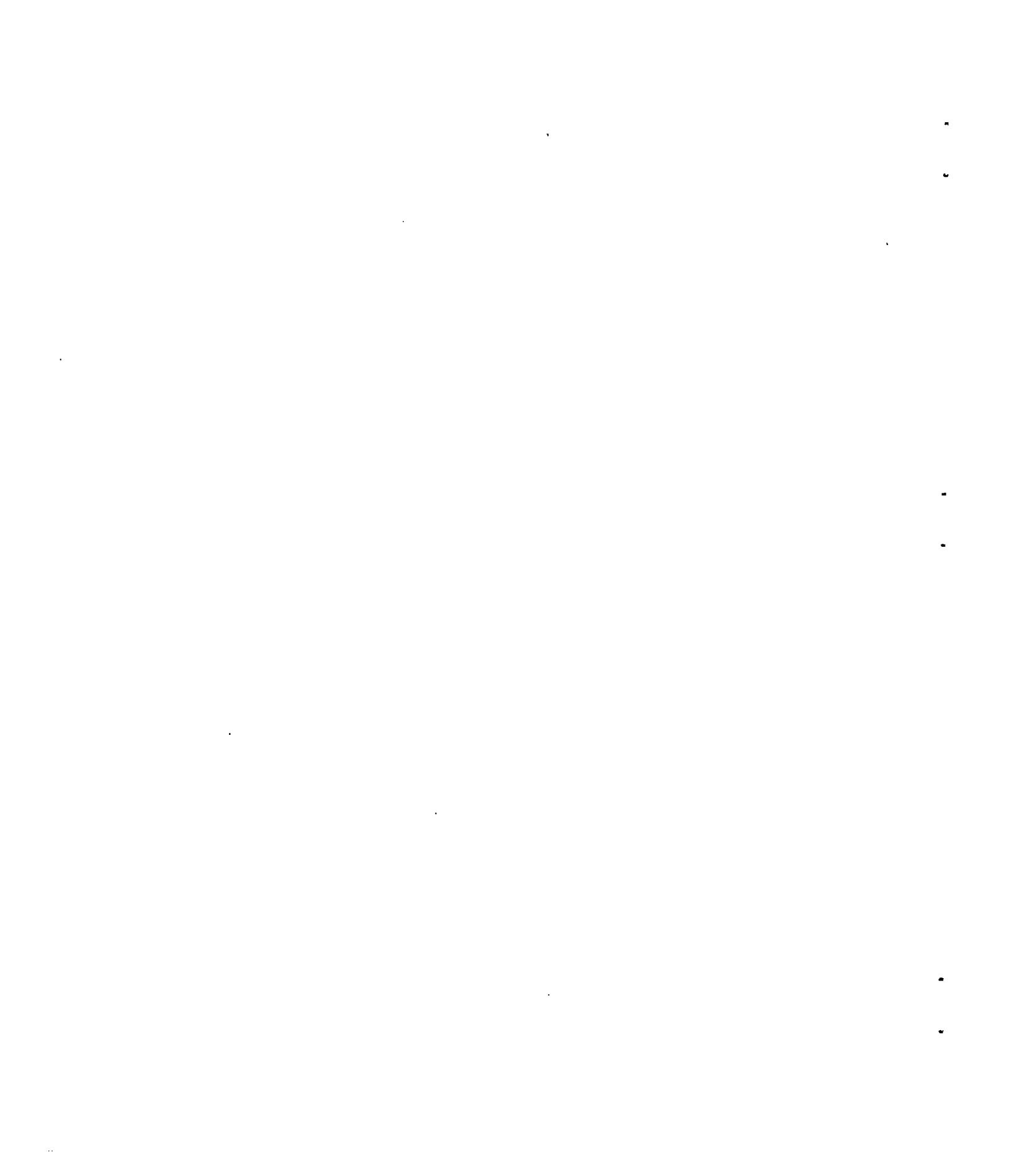
Figure 1.- Plan-form drawing of the A-, M-, and W-wings.





NACA  
L-64860.1

Figure 2.- Photograph of reflection-plane installation with W-wing mounted.



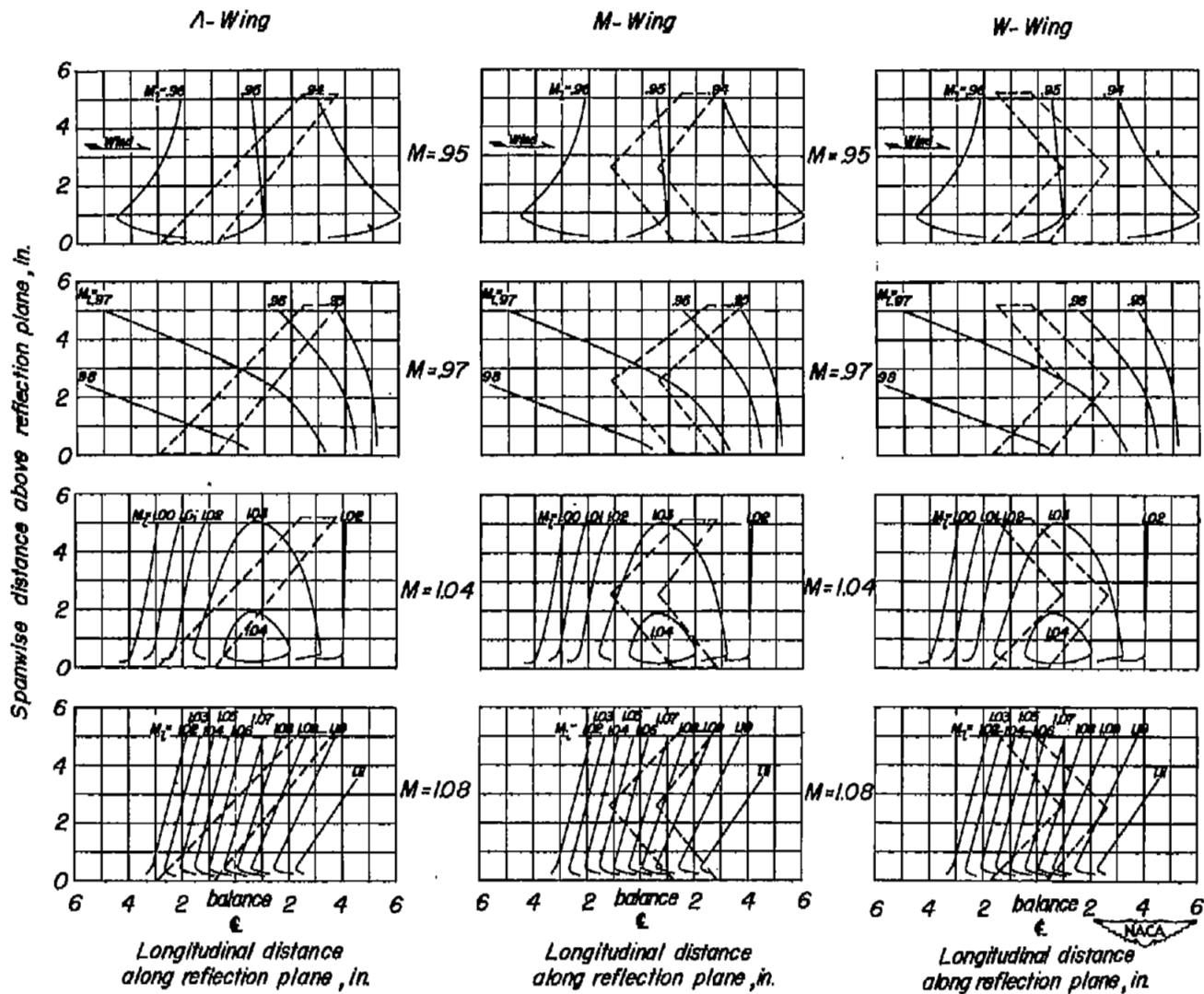


Figure 3.- Typical Mach number contours in the vicinity of the semispan models.

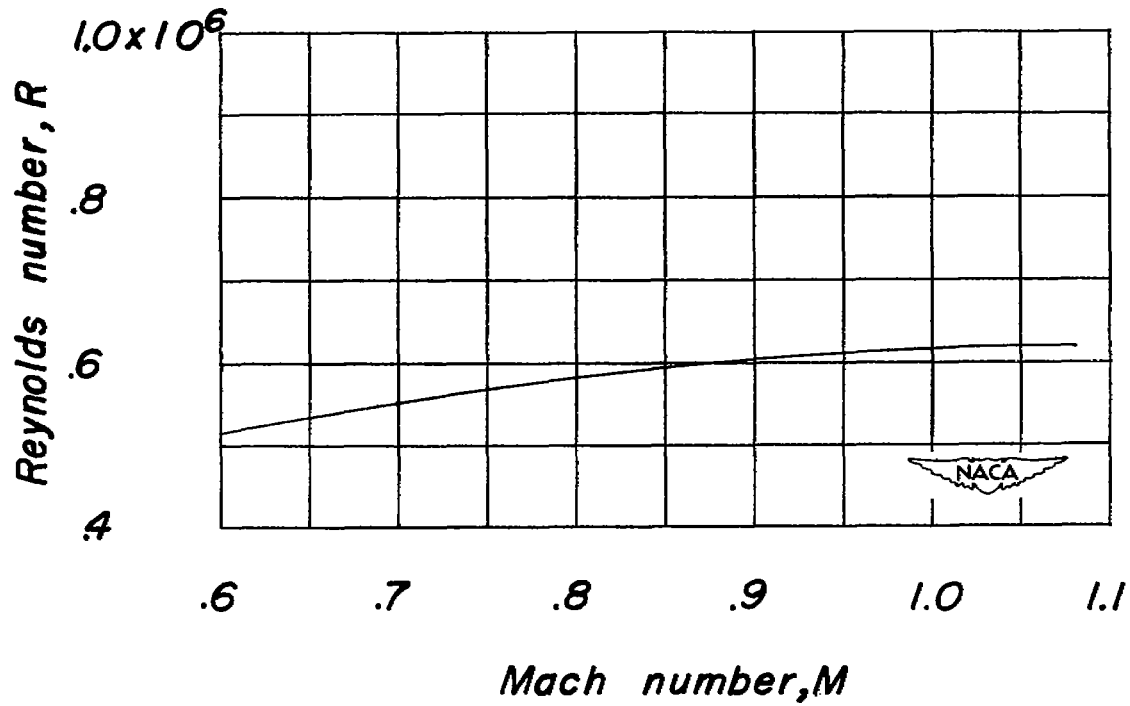


Figure 4.- Variation of average test Reynolds number with Mach number for the  $\Lambda$ -, M-, and W-wings.

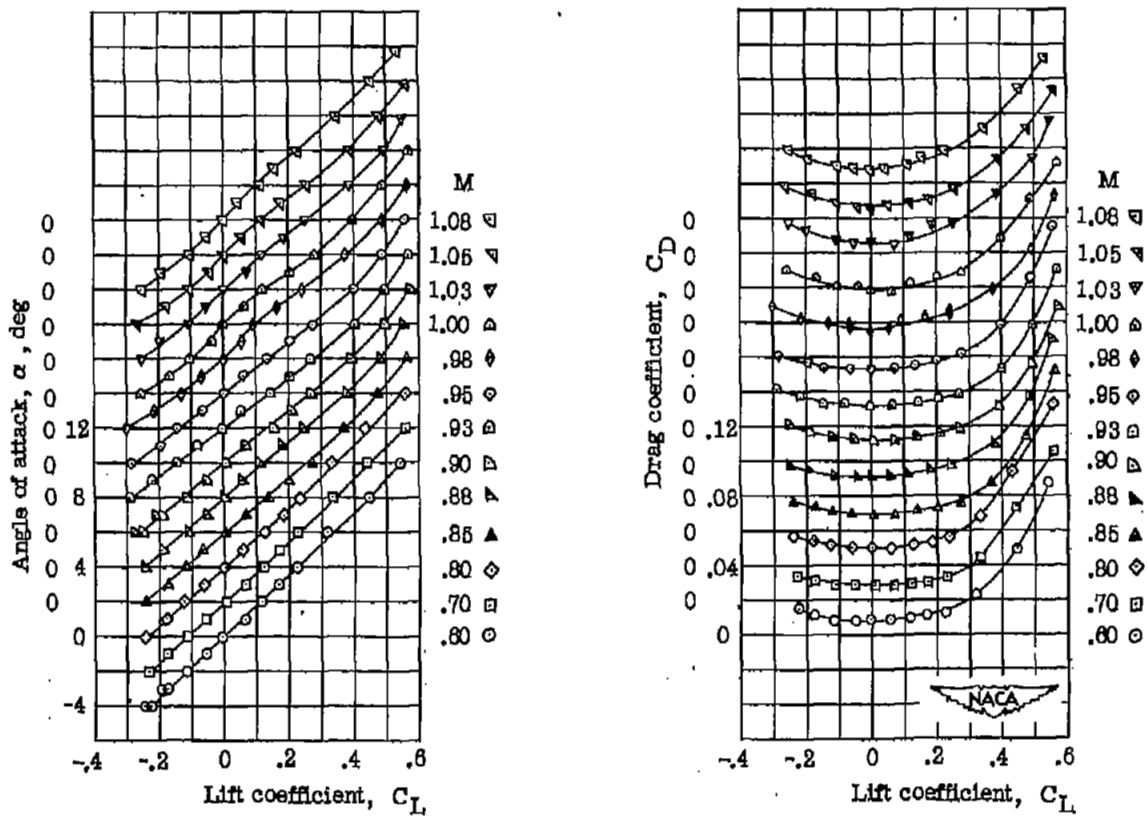


Figure 5.- Aerodynamic characteristics of a 45° sweptback wing having aspect ratio 6, taper ratio 0.6, and NACA 65A009 airfoil.

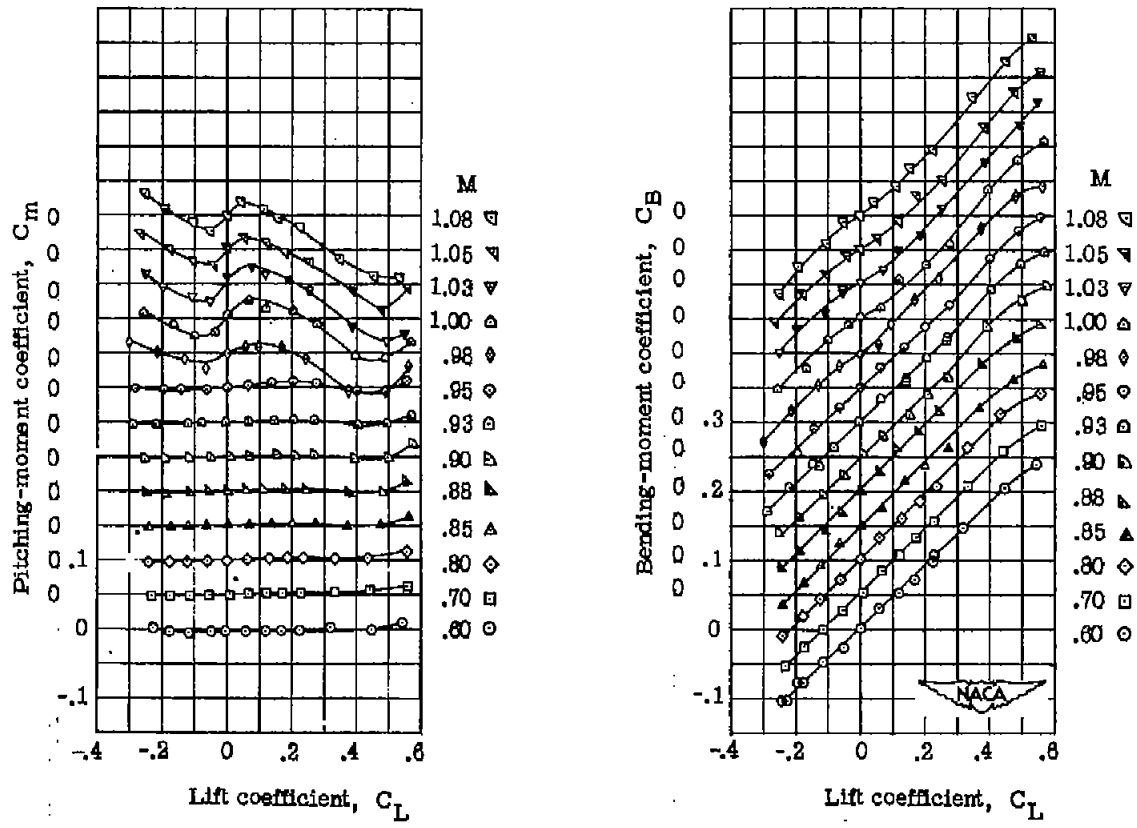


Figure 5.- Concluded.

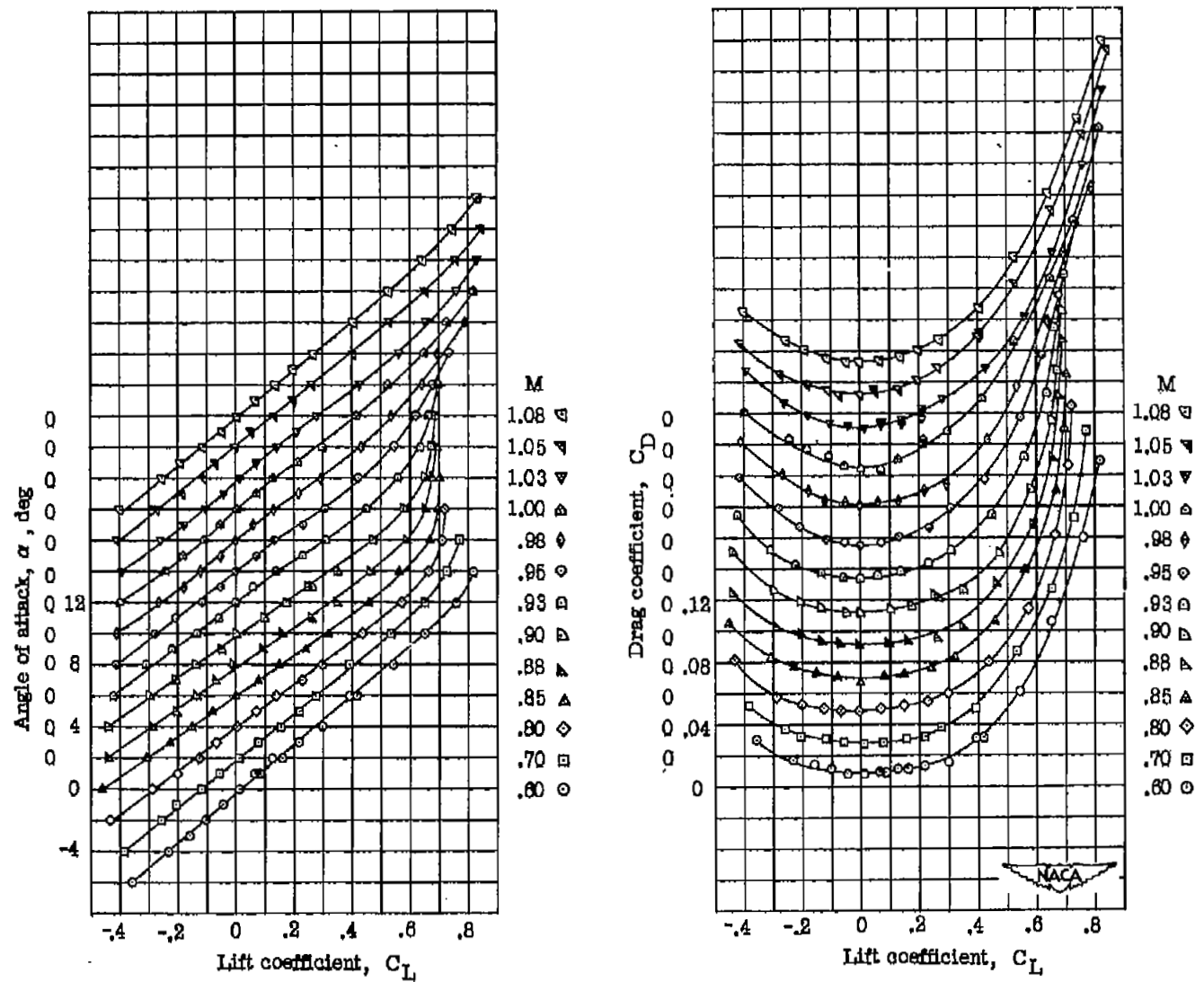


Figure 6.- Aerodynamic characteristics of an M-wing having  $45^\circ$  quarter-chord-panel sweep, aspect ratio 6, taper ratio 0.6, and NACA 65A009 airfoil.

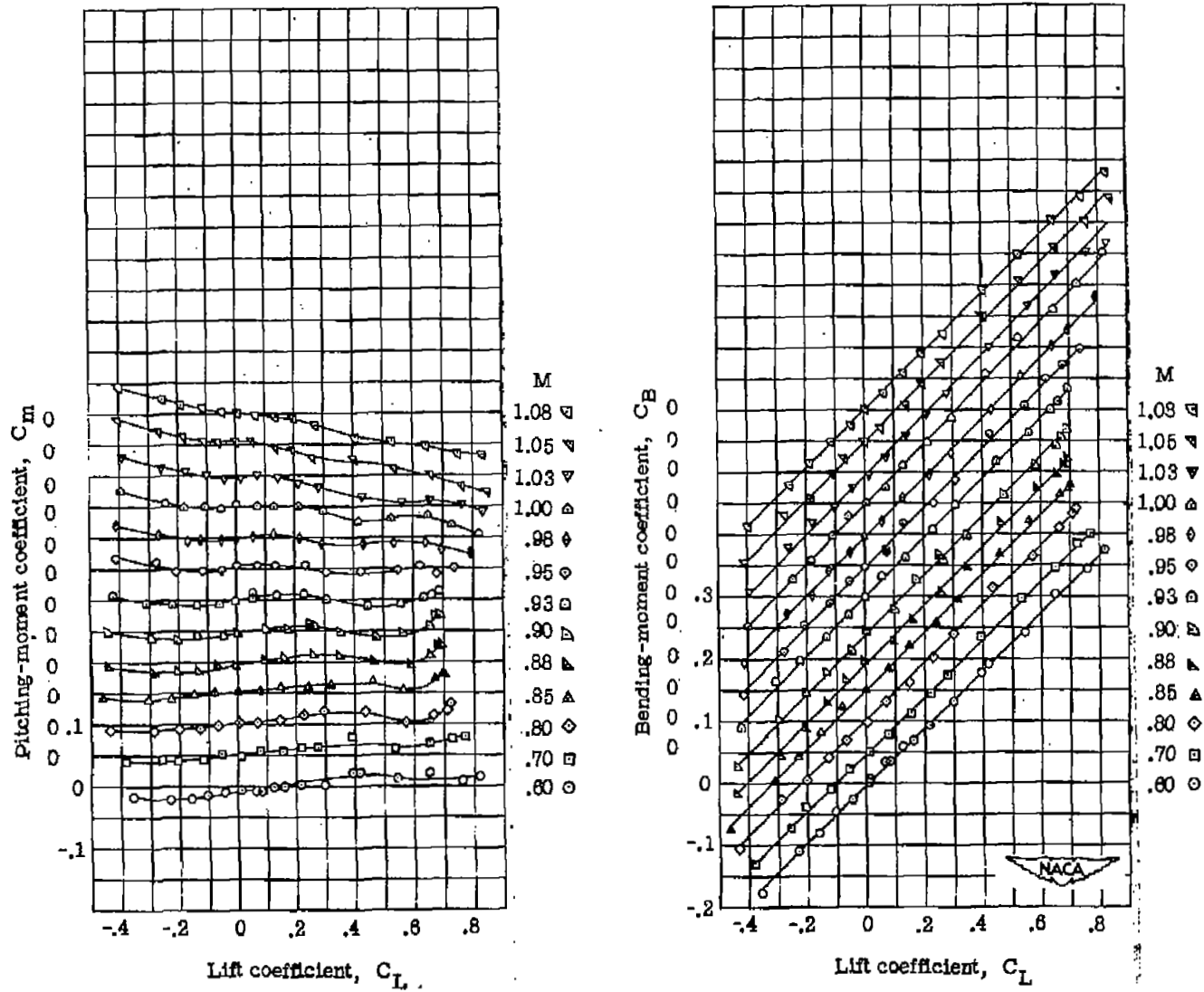


Figure 6.- Concluded.

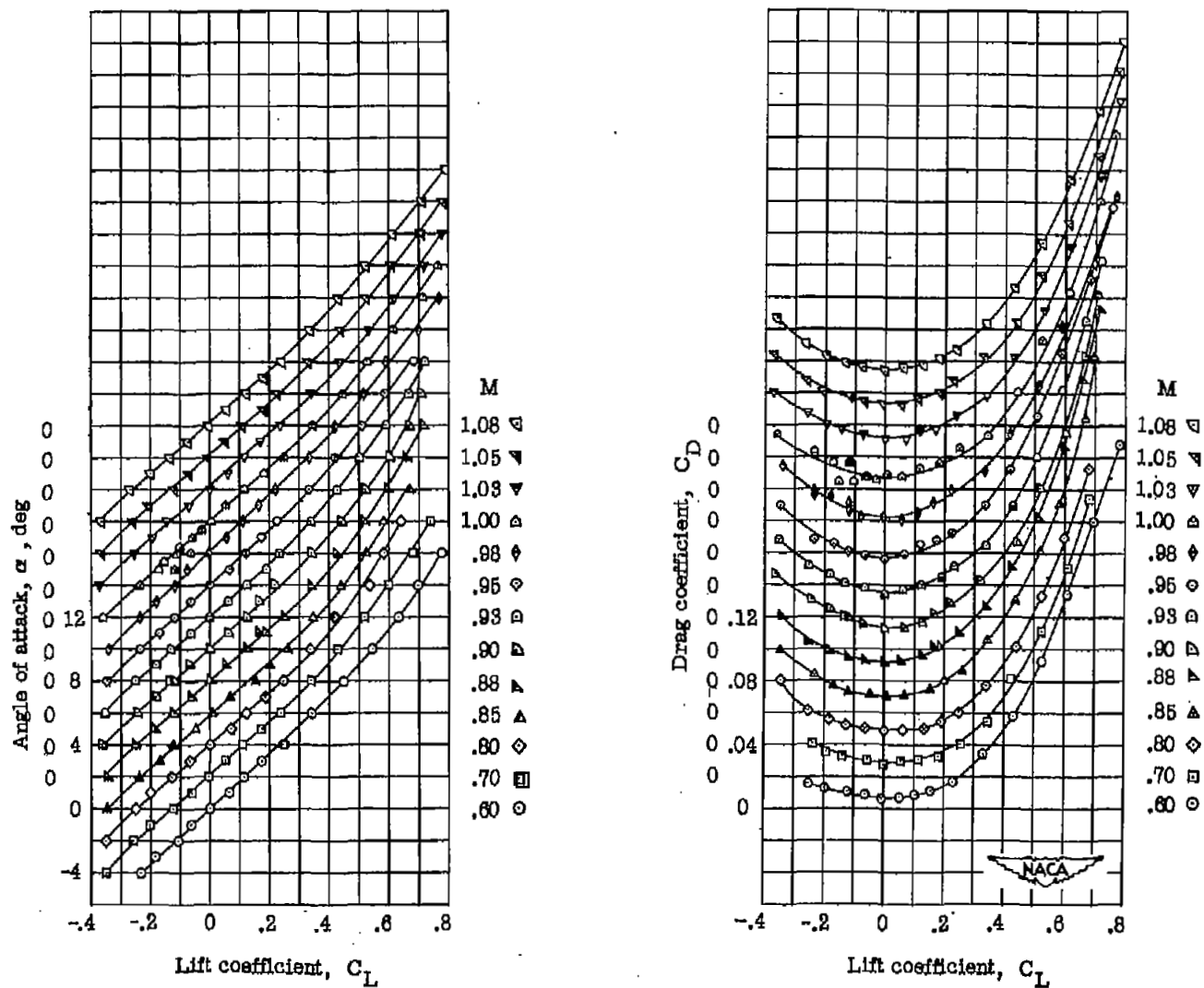


Figure 7.- Aerodynamic characteristics of a W-wing having  $45^\circ$  quarter-chord-panel sweep, aspect ratio 6, taper ratio 0.6, and NACA 65A009 airfoil.

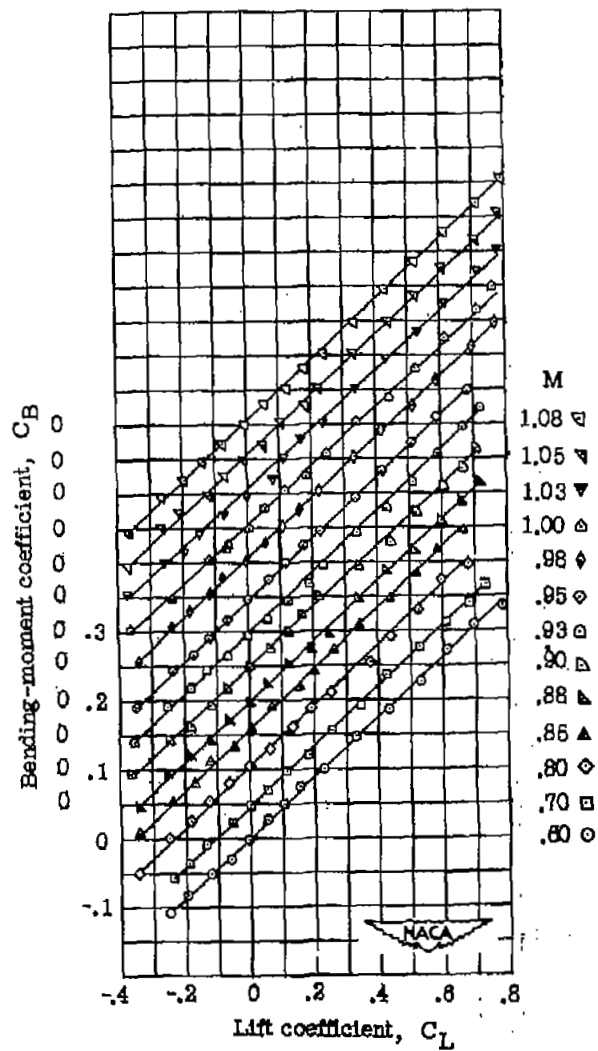
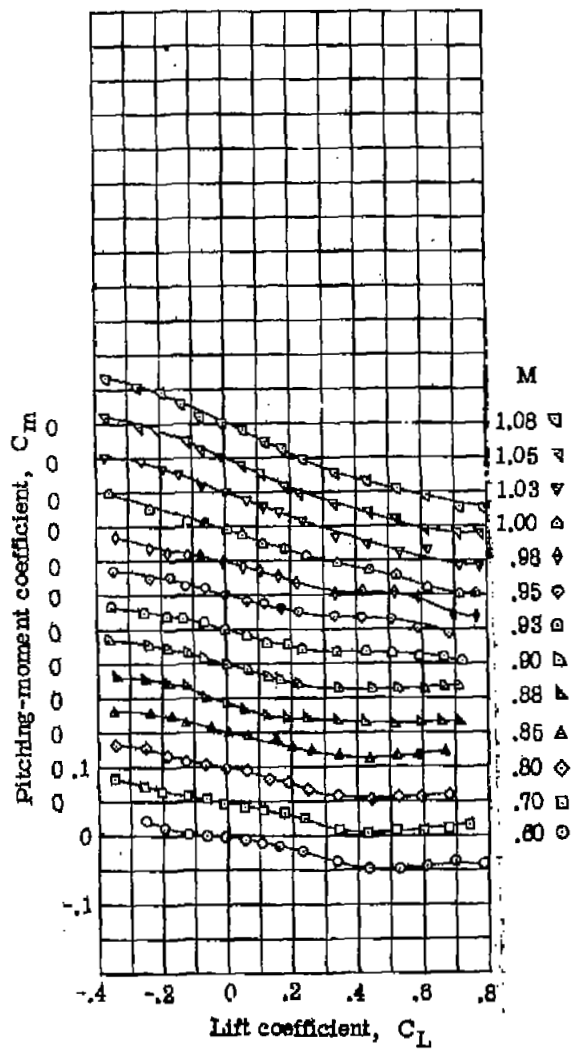


Figure 7.- Concluded.

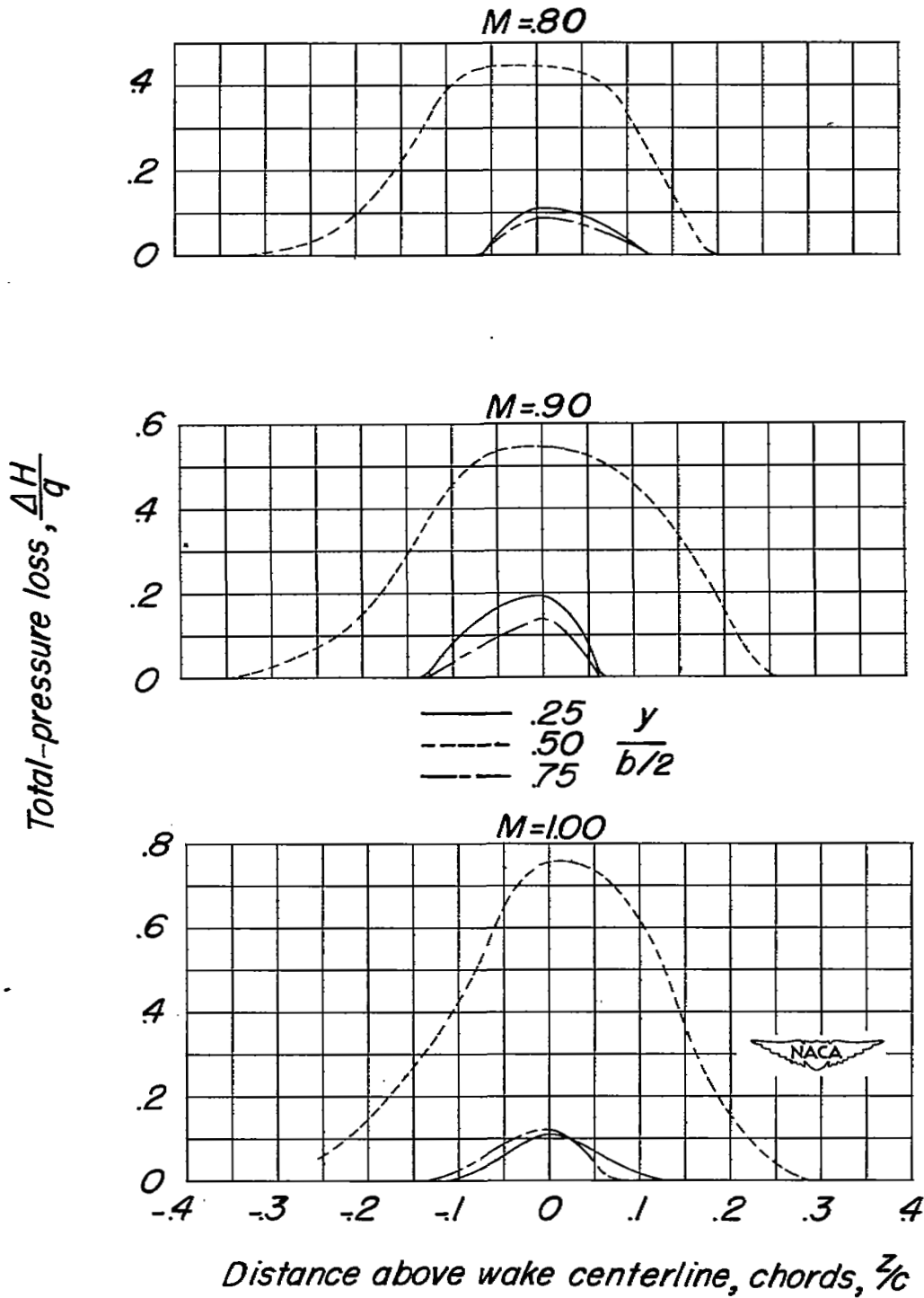
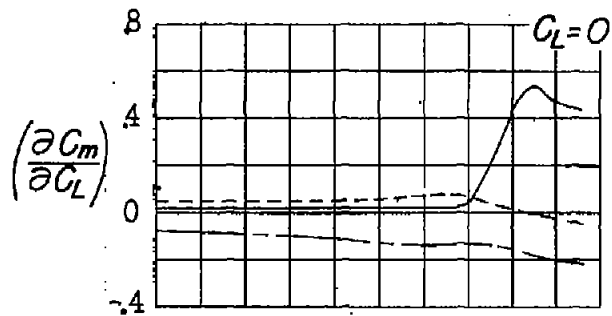
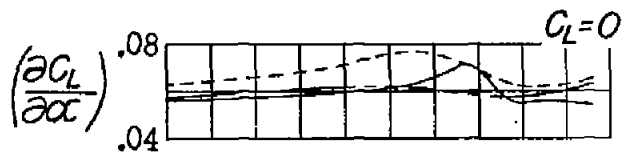


Figure 8.- Results of total-pressure surveys 4.2 inches behind quarter mean aerodynamic chord of W-wing.  $\alpha = 4^\circ$ .



Λ ———  
 M - - - -  
 W - · - · -

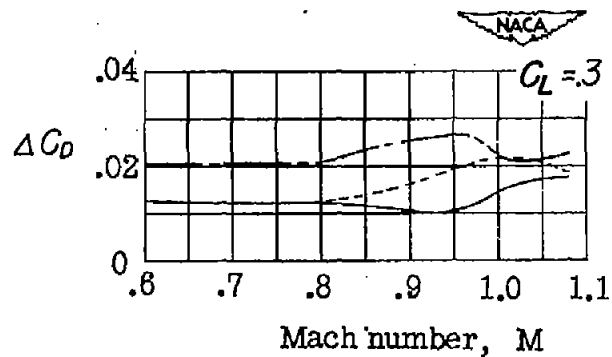
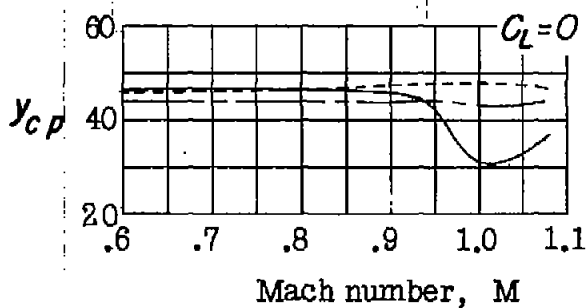
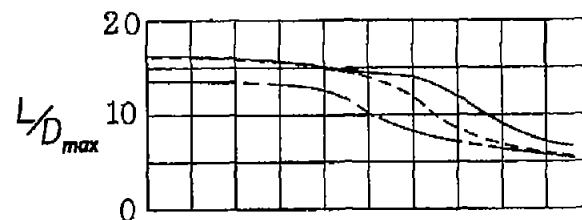


Figure 9.- Summary of aerodynamic characteristics of the Λ-, M-, and W-wings.

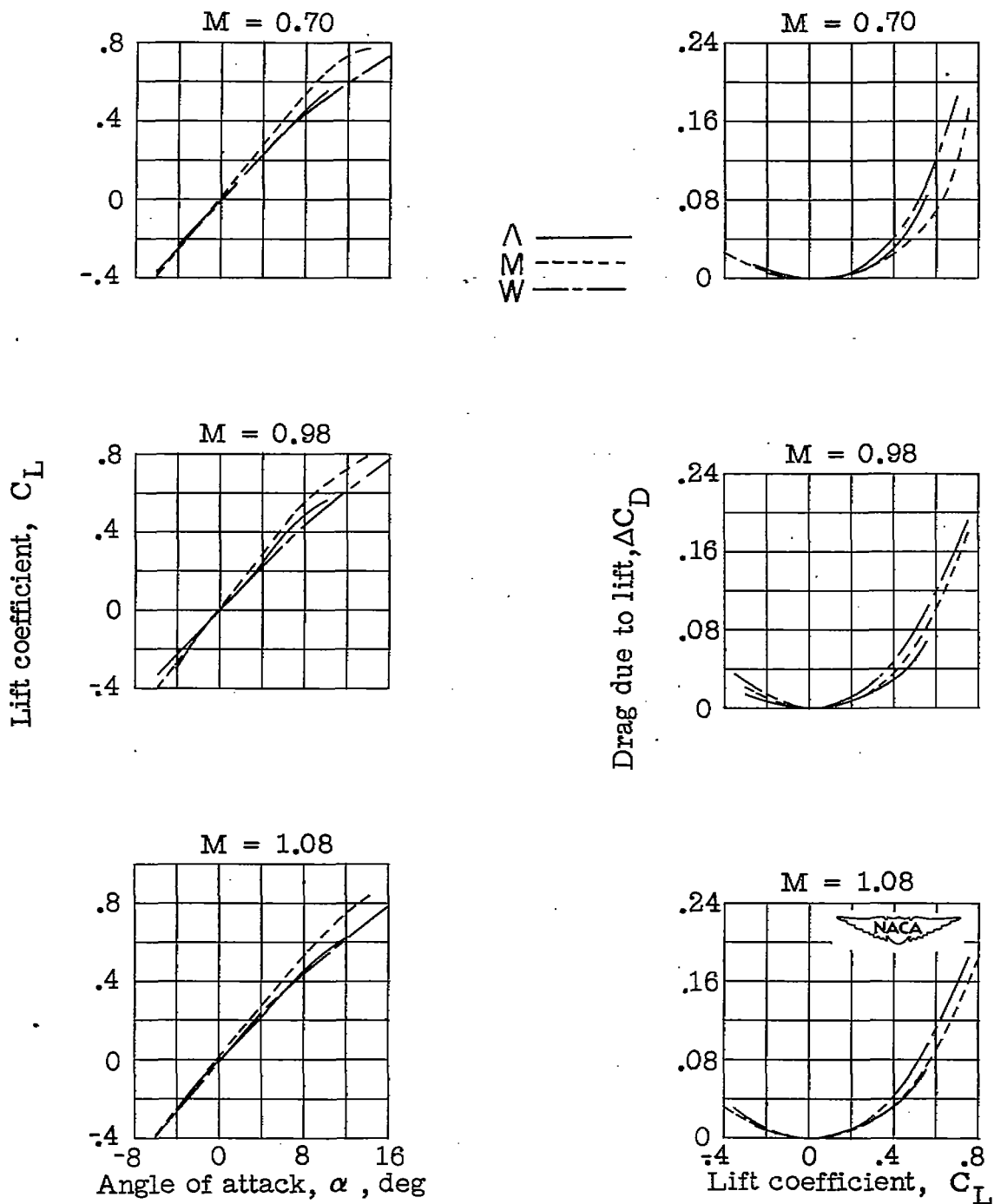


Figure 10.- Comparison of aerodynamic characteristics of  $\Lambda$ -, M-, and W-wings at representative Mach numbers.

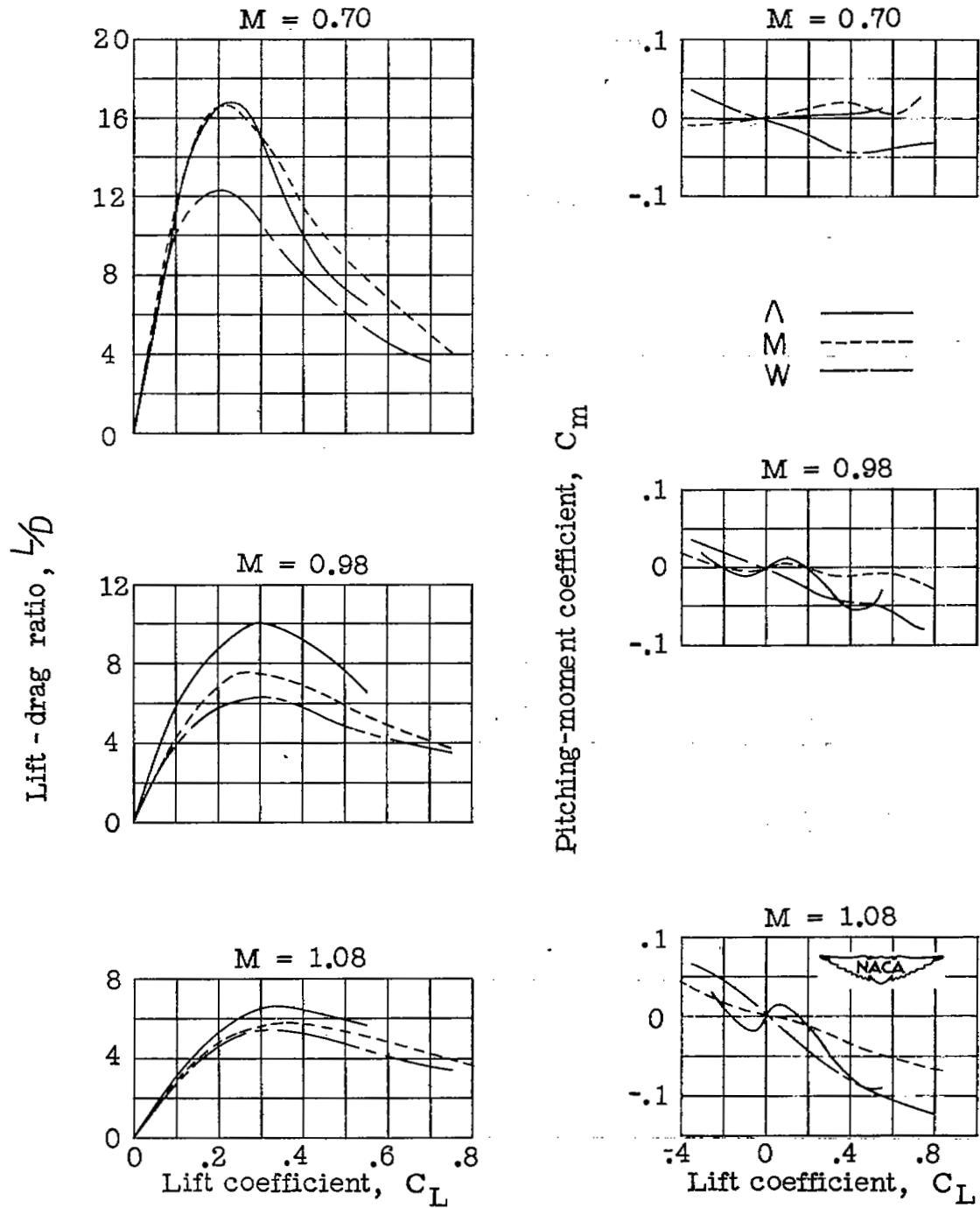


Figure 10.- Concluded.

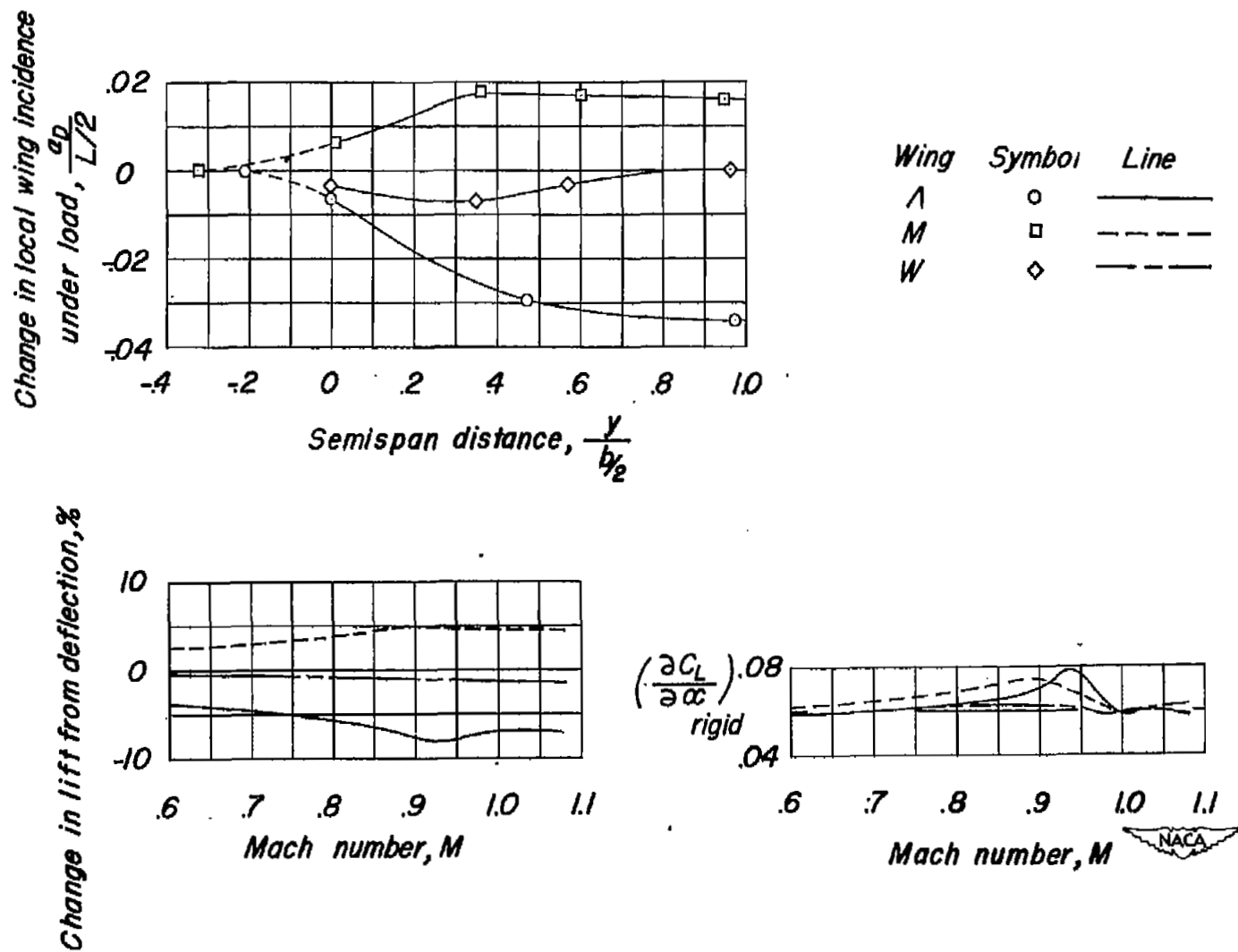


Figure 11.- Effects of wing deformation of A-, M-, and W-wings under static load.

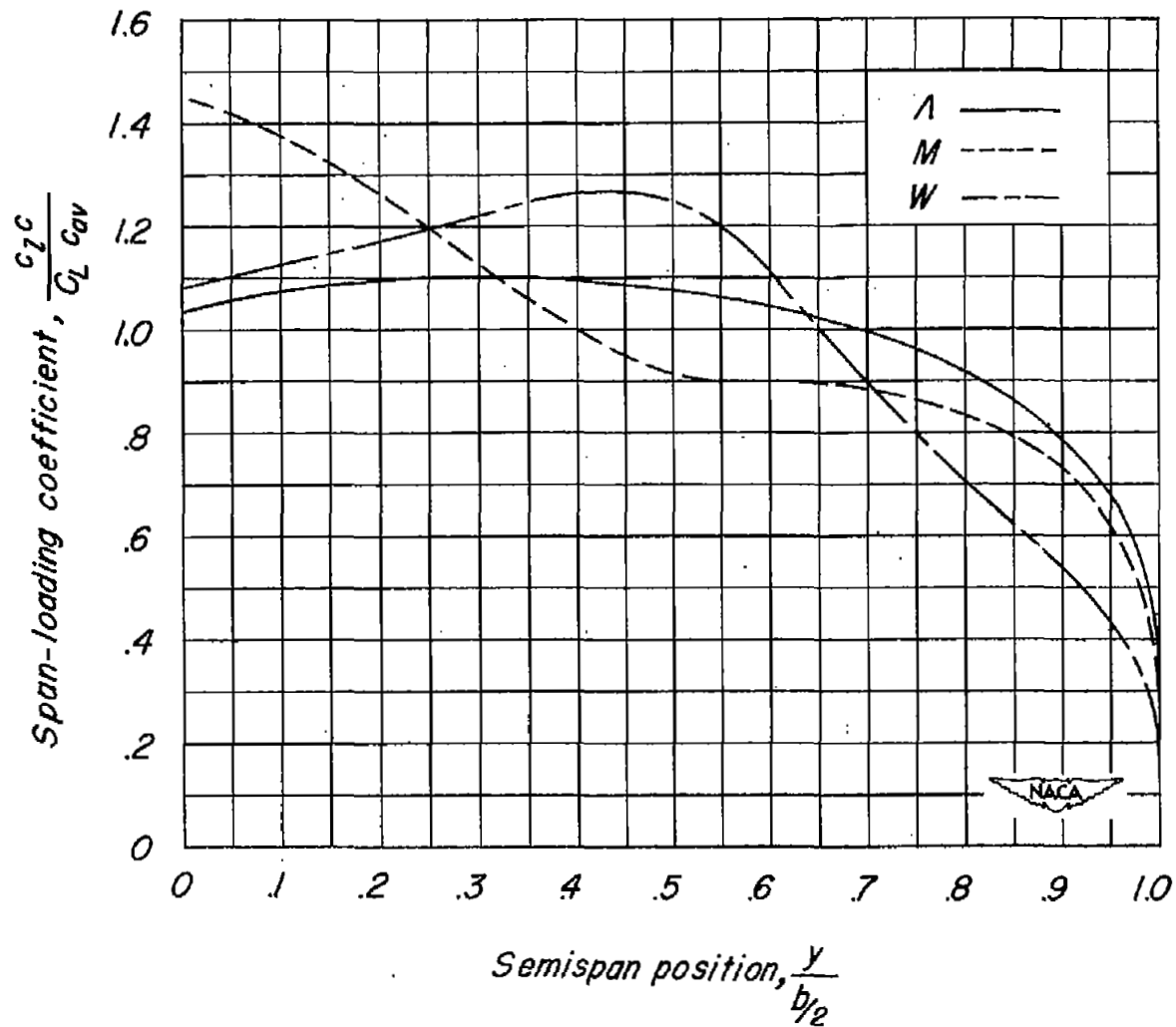


Figure 12.- Theoretical span loadings at a Mach number of 0.7 for  $\Lambda$ -, M-, and W-wings having  $45^\circ$  swept panels, aspect ratio 6, and 0.6 taper ratio.